Photoacoustic tomography to assess acute vasoactivity of systemic vasculature

Huda, Kristie, Lawrence, Dylan, Lindsey, Sarah, Bayer, Carolyn

Kristie Huda, Dylan Lawrence, Sarah Lindsey, Carolyn Bayer, "Photoacoustic tomography to assess acute vasoactivity of systemic vasculature," Proc. SPIE 11960, Photons Plus Ultrasound: Imaging and Sensing 2022, 1196007 (3 March 2022); doi: 10.1117/12.2612093

SPIE.

Event: SPIE BiOS, 2022, San Francisco, California, United States

Photoacoustic tomography to assess acute vasoactivity of systemic vasculature

Kristie Huda[a], Dylan Lawrence[a], Sarah Lindsey[b], Carolyn Bayer*[a]
[a]Dept. of Biomedical Engineering, Tulane University, 500 Lindy Boggs Center, New Orleans, LA 70118, USA
[b]Dept. of Pharmacology, Tulane University School of Medicine, 1430 Tulane Avenue, New Orleans, LA 70112, USA

ABSTRACT

Vasoactivity is an important physiological indicator of cardiovascular health which is frequently measured using *ex vivo* vessels to determine functional mechanisms and evaluate pharmacological responses. Currently, there are no imaging methods available to assess vasoactivity in multiple vascular beds of living animals noninvasively. In this work, we have developed methods to use photoacoustic tomography to assess vasoactivity *in vivo* in systemic vasculature of living animals. A spherical-view photoacoustic tomography system was used to monitor acute vasodilation in the whole abdomen of a pregnant mouse in response to injection of G-1. After 3D image reconstruction, the diameter of the iliac artery and photoacoustic signal intensity of a placenta over time was measured. The artery and placenta had differential response to the vasodilator G-1. We validated the observed vasodilation of artery by monitoring the change in cross-sectional diameter of an individual artery using standard B-mode ultrasound imaging.

Keywords: Photoacoustic tomography, placenta, vasodilation, GPER

1. INTRODUCTION

Vasoactivity is an important physiological indicator of cardiovascular health. Impaired vasoresponse to pharmacological or mechanical stimuli can indicate endothelial dysfunction which is associated with high cardiovascular risk and metabolic diseases like atherosclerosis[1], hypertension[2], peripheral arterial disease[3], diabetes[4], chronic kidney failure[5] etc. Vasoactivity is frequently measured using isolated vessels using wire or pressure myograph to determine functional mechanisms and evaluate pharmacological responses[6-8]. The limitations of these methods are that they are *ex vivo*, and may not represent the *in vivo* physiology, and that the laborious measurements are only practical for a single vessel or small selection of vessel anatomies. Noninvasive methods like high-resolution ultrasonography have been used for flow mediated vasodilation[9,10] or pulse wave velocity measurement for measuring arterial stiffness[11]. Although these methods are noninvasive, the measurement is applicable for single and superficial vessels. We sought to develop non-invasive imaging methods to assess vasoactivity in multiple vascular beds of living animals to provide a more complete representation of whole-body vascular function.

Photoacoustic imaging could be a potential imaging method to assess vasoactivity noninvasively. In photoacoustic imaging, nonionizing nanosecond pulses of light excite chromophores in the tissue, which induces thermoelastic expansion of chromophores and generates a broadband acoustic wave[12]. This acoustic wave can be detected using a broadband acoustic array transducer. This technique has been applied in oncology[13,14], angiogenesis[15,16], cardiovascular diseases[17-19] and ophthalmology[20-22]. Hemoglobin generates a very strong photoacoustic signal which can be used to visualize vascular anatomy within the body, including highly vascularized internal organs[16,23,24]. The generated photoacoustic signals can be acquired with tomographic systems which create 3D volumes. For example, we have previously used a spherical-view photoacoustic tomography system to capture anatomical structure of different vascular beds and function simultaneously[25]. These tomography systems can acquire 3D volumetric whole-body image of small animal in single rotation[23,26].

*carolynb@tulane.edu

Photons Plus Ultrasound: Imaging and Sensing 2022, edited by Alexander A. Oraevsky, Lihong V. Wang
Proc. of SPIE Vol. 11960, 1196007 · © 2022 SPIE · 1605-7422 · doi: 10.1117/12.2612093

In this work, we used the spherical-view photoacoustic tomography system to monitor the acute response of vasodilator G-1 in the systemic vasculature. G protein-coupled estrogen receptor (GPER) plays a role in estrogen-mediated protection of the cardiovascular system in women. G-1, a selective agonist of G protein-coupled estrogen receptor (GPER) causes endothelium-dependent vasodilation[27] and decreases blood pressure in ovariectomized rats[28]. The vasodilation observed with photoacoustic tomography was validated by monitoring the change in cross-sectional diameter of an individual artery using B-mode ultrasound imaging.

2. MATERIALS AND METHODS

To assess the ability of the photoacoustic tomography system to monitor acute vasoactivity, we used a timed pregnant CD-1 mouse at gestational day 16 following a protocol approved by the Tulane University Institutional Animal Care and Use Committee (IACUC). The animal was anesthetized by isoflurane (1-3%) mixed with oxygen gas (1-2 L/min). Before imaging, a jugular vein catheter was placed for the administration of vasodilators. Then the animal was transferred to the imaging platform and submerged in a deionized and degassed water bath heated to 36℃.

To demonstrate imaging of acute vasodilation, we administered G-1, a G protein-coupled estrogen receptor (GPER) agonist[8]. GPER agonist G-1 (100089335, Cayman Chemical, Ann Arbor, Michigan) was dissolved in 50% DMSO and 50% ethanol and diluted in PBS for administration. A volume of 0.1 mL at a dose of 100ug/kg of body weight followed by 0.1 mL saline was administered to the circulatory system through the right jugular vein catheter tube while imaging.

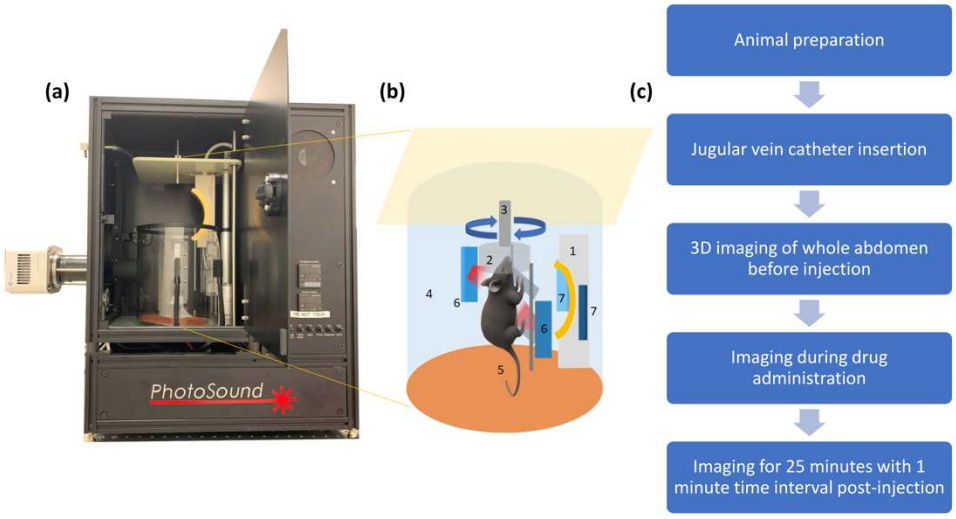

Figure 1. (a) A photoacoustic tomography system (TriTom). (b) A schematic diagram of photoacoustic tomography system. (1) Arc array transducer, (2) Animal holder with nose cone, (3) Anesthesia tube, (4) Imaging chamber, (5) Heating pad, (6,7) Optical fiber terminals. (c) Flow chart of experimental method.

A photoacoustic tomography system (TriTom, Photosound Inc., Houston, TX) (Figure 1(a)) with a 6 MHz central frequency arc array transducer was used to acquire all images of the mouse abdomen using a nanosecond pulsed tunable laser (Phocus HE, Opotek, Carlsbad, CA). A schematic diagram of the tomography system is shown in Figure 1(b). To illuminate the object of interest, two optical fiber terminals mounted in the imaging chamber at 90 degrees with respect to the vertical plane of the arc array transducer. The other two optical fiber terminals mounted at 45 degrees were placed to deliver light at 532 nm wavelength. A stepper motor was attached to the nose cone to rotate the object of interest mechanically while imaging. The field of view of the system was 30×30×30 mm, and a full image was acquired in 36 seconds. The 3D images were acquired before, during and after drug administration at 808 nm. As 808 nm is the isosbestic point of the optical absorption of hemoglobin and oxyhemoglobin, we used 808 nm for image acquisition. The images were reconstructed using a standard modified back-projection algorithm integrated with the TriTom system[29]. The speed of sound was adjusted for each scan to optimize the resolution of the reconstructed image. All the images were processed in Matlab (Mathworks, Natick, MA). The 3D images were then visualized in Amira (Thermo Fisher Scientific, Waltham, MA).

3. RESULTS

The change in diameter of the iliac artery and the change in the photoacoustic signal intensity of specific vascular features were measured to estimate the extent and temporal characteristics of the vasodilation. Figure 2(a) and (b) present the reconstructed 3D volume of PA image of mouse whole abdomen at gestational day 16 at 808 nm. The diameter of the artery was measured from the 2D slice of the sagittal plane of the artery using full width at half maximum, and the change of diameter vs. time is shown in figure 2(c). Figure 2(c) also shows the change in average PA signal intensity of the placenta vs. time, where PA signal intensity of the placenta was measured from a manually segmented 2D slice of the placenta. The imaging shows the peak vasodilation of the iliac artery at ~13 minutes post injection, while the PA signal intensity of the placental vasculature did not change over the observed time period.

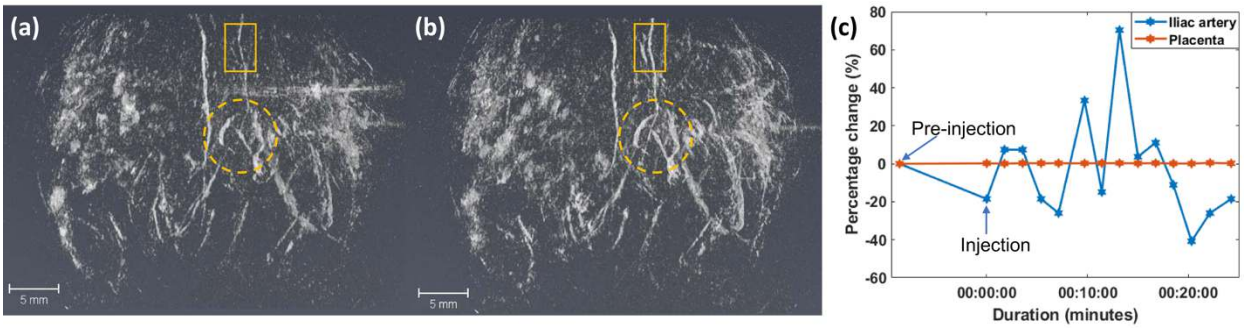

Figure 2. Visualization of 3D photoacoustic tomography image of whole abdomen of a pregnant mouse at 808 nm (a) pre-injection and (b) 13 minutes post-injection. (c) Plot of change in diameter of iliac artery (blue color) and plot of change in average photoacoustic (PA) signal intensity (orange color) vs. duration. The yellow box indicates iliac artery and yellow circle indicates the placenta in (a) and (b). Scare bar is 5 mm.

4. CONCLUSION

In this work, we demonstrated the ability to monitor systemic acute vasodilation *in vivo* using photoacoustic tomography imaging. The iliac artery showed a similar time response of peak vasodilation as the cross-sectional change in diameter of an individual artery using standard B-mode ultrasound imaging. On the other hand, the placenta manifested a different response to the vasodilator, when compared to the response of the artery. In future work, these methods can be used to assess differential systemic responses to vasoactive therapies.

REFERENCES

[1] Sitia, S., Tomasoni, L., Atzeni, F., Ambrosio, G., Cordiano, C., Catapano, A., Tramontana, S., Perticone, F., Naccarato, P., Camici, P., Picano, E., Cortigiani, L., Bevilacqua, M., Milazzo, L., Cusi, D., Barlassina, C., Sarzi-Puttini, P., Turiel, M., "From endothelial dysfunction to atherosclerosis," Autoimmunity Reviews 9(12), 830-834 (2010).

[2] Park, J., Charbonneau, F., Schiffrin, E., "Correlation of endothelial function in large and small arteries in human essential hypertension.," Journal of Hypertension 19(3), 415-420 (2001).

[3] Vita, J. A., Hamburg, N. M., "Does endothelial dysfunction contribute to the clinical status of patients with peripheral arterial disease?," Can J Cardiol 26 Suppl A(45A-50A (2010).

[4] Calles-Escandon, J., Cipolla, M., "Diabetes and endothelial dysfunction: a clinical perspective," Endocr Rev 22(1), 36-52 (2001).

[5] Zoccali, C., "The endothelium as a target in renal diseases," J Nephrol 20 Suppl 12(S39-44 (2007).

[6] Bevan, J. A., Osher, J. V., "A direct method for recording tension changes in the wall of small blood vessels in vitro," Agents Actions 2(5), 257-260 (1972).

[7] Halpern, W., Osol, G., Coy, G. S., "Mechanical behavior of pressurized in vitro prearteriolar vessels determined with a video system," Ann Biomed Eng 12(5), 463-479 (1984).

[8] Lindsey, S., Carver, K., Prossnitz, E., Chappell, M., "Vasodilation in Response to the GPR30 Agonist G-1 is Not Different From Estradiol in the mRen2.Lewis Female Rat," Journal of Cardiovascular Pharmacology 57(5), 598-603 (2011).

[9] Celermajer, D. S., Sorensen, K. E., Gooch, V. M., Spiegelhalter, D. J., Miller, O. I., Sullivan, I. D., Lloyd, J. K., Deanfield, J. E., "Non-invasive detection of endothelial dysfunction in children and adults at risk of atherosclerosis," Lancet 340(8828), 1111-1115 (1992).
[10] Schuler, D., Sansone, R., Freudenberger, T., Rodriguez-Mateos, A., Weber, G., Momma, T., Goy, C., Altschmied, J., Haendeler, J., Fischer, J., Kelm, M., Heiss, C., "Measurement of Endothelium-Dependent Vasodilation in Mice-Brief Report," Arteriosclerosis Thrombosis and Vascular Biology 34(12), 2651-U2176 (2014).
[11] Laurent, S., Cockcroft, J., Van Bortel, L., Boutouyrie, P., Giannattasio, C., Hayoz, D., Pannier, B., Vlachopoulos, C., Wilkinson, I., Struijker-Boudier, H., Arteries, E. N. f. N.-i. I. o. L., "Expert consensus document on arterial stiffness: methodological issues and clinical applications," Eur Heart J 27(21), 2588-2605 (2006).
[12] Xia, J., Yao, J., Wang, L. V., "Photoacoustic tomography: principles and advances," Electromagn Waves (Camb) 147(1-22 (2014).
[13] Li, M., Oh, J., Xie, X., Ku, G., Wang, W., Li, C., Lungu, G., Stoica, G., Wang, L., "Simultaneous molecular and hypoxia imaging of brain tumors in vivo using spectroscopic photoacoustic tomography," Proceedings of the Ieee 96(3), 481-489 (2008).
[14] Lungu, G., Li, M., Xie, X., Wang, L., Stoica, G., "In vivo imaging and characterization of hypoxia-induced neovascularization and tumor invasion.," Journal of Nutrition 137(1), 278S-279S (2007).
[15] Ku, G., Wang, X., Xie, X., Stoica, G., Wang, L., "Imaging of tumor angiogenesis in rat brains in vivo by photoacoustic tomography," Applied Optics 44(5), 770-775 (2005).
[16] Kruger, R. A., Lam, R. B., Reinecke, D. R., Del Rio, S. P., Doyle, R. P., "Photoacoustic angiography of the breast," Med Phys 37(11), 6096-6100 (2010).
[17] Karlas, A., Fasoula, N., Paul-Yuan, K., Reber, J., Kallmayer, M., Bozhko, D., Seeger, M., Eckstein, H., Wildgruber, M., Ntziachristos, V., "Cardiovascular optoacoustics: From mice to men - A review," Photoacoustics 14(19-30 (2019).
[18] Zemp, R., Song, L., Bitton, R., Shung, K., Wang, L., "Realtime Photoacoustic Microscopy of Murine Cardiovascular Dynamics," Optics Express 16(22), 18551-18556 (2008).
[19] Taruttis, A., Herzog, E., Razansky, D., Ntziachristos, V., "Real-time imaging of cardiovascular dynamics and circulating gold nanorods with multispectral optoacoustic tomography," Optics Express 18(19), 19592-19602 (2010).
[20] Hu, S., Rao, B., Maslov, K., Wang, L., "Label-free photoacoustic ophthalmic angiography," Optics Letters 35(1), 1-3 (2010).
[21] de la Zerda, A., Paulus, Y., Teed, R., Bodapati, S., Dollberg, Y., Khuri-Yakub, B., Blumenkranz, M., Moshfeghi, D., Gambhir, S., "Photoacoustic ocular imaging," Optics Letters 35(3), 270-272 (2010).
[22] Hennen, S., Xing, W., Shui, Y., Zhou, Y., Kalishman, J., Andrews-Kaminsky, L., Kass, M., Beebe, D., Maslov, K., Wang, L., "Photoacoustic tomography imaging and estimation of oxygen saturation of hemoglobin in ocular tissue of rabbits," Experimental Eye Research 138(153-158 (2015).
[23] Ermilov, S., Su, R., Conjusteau, A., Anis, F., Nadvoretskiy, V., Anastasio, M., Oraevsky, A., "Three-Dimensional Optoacoustic and Laser-Induced Ultrasound Tomography System for Preclinical Research in Mice: Design and Phantom Validation," Ultrasonic Imaging 38(1), 77-95 (2016).
[24] Li, C., Aguirre, A., Gamelin, J., Maurudis, A., Zhu, Q., Wang, L., "Real-time photoacoustic tomography of cortical hemodynamics in small animals," Journal of Biomedical Optics 15(1), (2010).
[25] Huda, K., Wu, C., Sider, J., Bayer, C., "Spherical-view photoacoustic tomography for monitoring in vivo placental function," Photoacoustics 20((2020).
[26] Brecht, H., Su, R., Fronheiser, M., Ermilov, S., Conjusteau, A., Oraevsky, A., "Whole-body three-dimensional optoacoustic tomography system for small animals," Journal of Biomedical Optics 14(6), (2009).
[27] Fredette, N., Meyer, M., Prossnitz, E., "Role of GPER in estrogen-dependent nitric oxide formation and vasodilation," Journal of Steroid Biochemistry and Molecular Biology 176(65-72 (2018).
[28] Lindsey, S., Cohen, J., Brosnihan, K., Gallagher, P., Chappell, M., "Chronic Treatment with the G Protein-Coupled Receptor 30 Agonist G-1 Decreases Blood Pressure in Ovariectomized mRen2.Lewis Rats," Endocrinology 150(8), 3753-3758 (2009).
[29] Xu, M., Wang, L., "Time-domain reconstruction for thermoacoustic tomography in a spherical geometry," Ieee Transactions on Medical Imaging 21(7), 814-822 (2002).